Sex Plant Reprod (1998) 11:121–130

ORIGINAL PAPER

T.N. Naumova · F. Matzk

Differences in the initiation of the zygotic and parthenogenetic pathway in the Salmon lines of wheat: ultrastructural studies

Received: 25 November 1997 / Revision accepted: 16 April 1998

Abstract The ultrastructure of the egg apparatus of the sexual (*aestivum*)-Salmon line (aS) and the isogenic but alloplasmic (*kotschyi*)-Salmon line (kS) of the Salmon system of wheat was studied by transmission electron microscopy 3 days before and during anthesis. Additionally, the zygotic stage of aS, 17 h after pollination, was included. Metabolic activity of egg cells from the sexual line aS was low 3 days before anthesis and increased dramatically after pollination and fertilization. This timing of increased activity was evident because of changes occurring in the egg cell nucleus and nucleolus, polysomes, endoplasmic reticulum and Golgi apparatus, and the completion of the cell wall around the zygote. In contrast to the sexual line, the egg cell of the parthenogenetic line showed high activity 3 days before anthesis. The metabolic and ultrastructural characters observed in the nucleus and cytoplasm of the kS line 3 days before and during anthesis corresponded with those of the isogenic sexual line aS during anthesis and 17 h after pollination, respectively. High metabolic activity observed in the persistent synergid of kS may be connected with the occurrence of additional embryos in seeds (twins) of this line.

Key words Egg cell · Parthenogenesis · Synergid · Ultrastructure · Wheat · Zygote

Introduction

Apomixis offers the potential for fixation of heterosis. However, to harness apomixis for agriculture, more knowledge is needed about the cellular and molecular events that control the individual steps of apomictic seed formation. In contrast to the meiotic/zygotic pathway in sexual plants, embryogenesis in apomictic plants follows an apomeiotic/parthenogenetic pathway. The two types of apomeiosis - apospory and diplospory - have been analysed by ultrastructural studies in several Poaceae (Naumova 1993; Naumova et al. 1993; Naumova and Willemse 1995; Osadtchiy and Naumova 1996). Such data are lacking for parthenogenesis in apomictic species. There is only limited data concerning the autonomous embryo development of reduced egg cells from a barley mutant (Mogensen 1982) and from in vitro culture of ovules from sexually reproducing sunflowers (Yan et al. 1989).

The Salmon system of wheat provides a suitable model system for studying the transition from the gametophytic to the sporophytic generation in vivo by comparing the initiation of embryo development in sexual and parthenogenetic isogenic lines (Matzk 1996). The genetic characteristics associated with haploid parthenogenesis of the alloplasmic Salmon lines were described by Tsunewaki and Mukai (1990). We improved the system and increased the parthenogenetic capacity from originally 20% to 90% in both isogenic lines (*caudata*)-Salmon and (*kotschyi*)-Salmon (Matzk et al. 1995). Autonomous embryo development was independent of fertilization of the polar nuclei as shown by the auxin test and by pollination experiments before and after anthesis. Although initiation of parthenogenesis probably began before or during anthesis, the highest capacity was realized during anthesis. Twins were formed at a frequency of about 20%. The twin plants usually had different ploidy levels; one was haploid (parthenogenetic pathway) and the other diploid (zygotic pathway). On the molecular level, there were only small differences between the three isogenic but alloplasmic lines (Bäumlein et al. 1996; Matzk et al. 1995). However, one embryo-sac-specific α-tubulin probably involved in initiation of embryo formation in the parthenogenetic lines could be identified (Matzk et al. 1997).

In this work, we compare the ultrastructure of the egg apparatus in the sexual line with that of the parthenoge-

T.N. Naumova[1] · F. Matzk (✉)
Institut für Pflanzengenetik und Kulturpflanzenforschung (IPK), Corrensstrasse 3, D-06466 Gatersleben, Germany
e-mail: matzk@ipk-gatersleben.de;
Fax: 039482–5137 or 039482–280

[1] *Present address*: Komarov Botanical Institute, Russian Academy of Sciences, St. Petersburg, Russia

netic isogenic line before and during anthesis and discuss these results with respect to the molecular, cytological, and phenotypical data already obtained for this model system.

Materials and methods

Plant material

Plants of the two lines (*kotschyi*)-Salmon (kS) and (*aestivum*)-Salmon (aS) were grown in pots in the greenhouse with a 16-h photoperiod and day/night temperatures around 22/12°C during the reproductive phase. Only the amphidiploid plants (2n=42) were used from the parthenogenetic line kS. Polyhaploid seedlings (2n=21) were eliminated after determination of ploidy level of leaf cell nuclei by flow cytometry.

To study cellular events associated with the initiation of embryo development, three ovaries were analysed from the parthenogenetic and sexual lines 3 days before and during anthesis, respectively. Developmental stages of the ovaries were determined for the individual florets of a spike; only the upper two florets of each spikelet were considered. Ovules from both lines were fixed for each stage between 9:00 a.m. and 10:30 a.m. The stage 3 days before anthesis was calculated as 10 days after the first meiotic division, which was determined in pollen mother cells of both lines by microscopic inspection. Anthesis occurred 13 days after meiosis in our experiments. Anthesis was defined in both lines as the time individual florets were opening, which is characterized by swelling of the lodicule and spreading of the feathery stigma. It corresponds to 30 min before to 30 min after self-pollination in the sexual male-fertile plants. Ovaries of the kS line were unpollinated during anthesis because the line is male sterile. Additionally, ovules of the sexual line were fixed 17 h after pollination to compare the phases of highest activity of egg cell/zygote; for this experiment, florets were emasculated and hand-pollinated. Single ovules of each line were analysed 3 days after anthesis to confirm parthenogenetic and sexual embryo formation. This time frame was the same one used for cytological and molecular studies by Matzk et al. (1995, 1997).

TEM technique

Ovules were dissected from ovaries and fixed in 3.5% glutaraldehyde in 0.05 M cacodylate buffer at pH 7.2 for 4 h at room temperature; this was followed by three buffer rinses. The ovules were then postfixed overnight with 2% OsO_4 in 0.025 M cacodylate buffer, dehydrated in an acetone series and embedded in eponaraldite embedding medium. Ultrathin sections were made with a diamond knife on a Reichert Ultracat-S ultramicrotome and poststained with uranyl acetate and Reynold's lead citrate. Semi-thin sections were stained with toluidine blue. An Amplival light microscope and ZEISS-902 transmission electron microscope were used for these investigations.

Results

Ultrastructural characteristics of the egg apparatus in the sexual line (*aestivum*)-Salmon

Three days before anthesis

The egg cell was round and larger than the synergids. The spherical nucleus occupied a central position within the egg cell (Fig. 1A). The chromatin structure of the nucleus was rather homogenous. No dense heterochromatin was observable. The nuclear envelope revealed relatively few pores. A few ribosomes were attached to the outer nuclear membrane (Fig. 1B). The nucleolus was large, contained numerous nucleolar vacuoles and the granular component predominated (Fig. 1C).

In the cytosol of the egg cell, most organelles were situated close to the nucleus. Vacuoles occupied the cell periphery (Fig. 1A). The cytoplasm contained a relatively small number of free ribosomes and a few polysomes. The endoplasmic reticulum (ER) of the short cisternal phase sporadically extended through the cytosol. ER membranes were rarely associated with ribosomes (Fig. 1B). The plasma membrane was flat. Plastids and mitochondria were numerous. Plastid stroma appeared less transparent than the mitochondrial matrix. Starch granules occurred in plastids (Fig. 1B). The internal mitochondrial matrix formed a number of cristae (Fig. 1B). Lipid bodies were distributed randomly in the cytosol. The cell wall of the egg cell appeared thick at the micropylar end and was thin and partly interrupted by a plasma membrane at the chalazal region (Fig. 1D).

The synergids were pyriform. The receptive synergid was already in the process of degradation. The cell organelles tended to aggregate but the membranes of the individual organelles were still discernible. Large vacuoles appeared in various parts of the cell. Processes of degeneration were less pronounced in the persistent synergid: the cell organelles were still intact but a large amount of lipid was already present in the cell (Fig. 1E).

Table 1 Characteristics of the egg apparatus of the sexual (aS) and parthenogenetic (kS) Salmon lines of wheat before and during anthesis. Three embryo sacs from each line were examined at each stage

Stage and characteristic	aS	kS
Three days before anthesis		
Egg cell diameter, μm	~43	~75
Egg cell surface (median plane), μm^2	~1900	~4400
Metabolic activity of egg cell	Low	High
Cell wall of chalazal part	Partly interrupted	Absent
Persistent synergid	Degradation beginning	Metabolic activity
During anthesis		
Egg cell diameter, μm	~76	~80
Egg cell surface (median plane), μm^2	~4200	~5000
Metabolic activity of egg cell	High	Very high
Cell wall of chalazal part	Absent	Absent
Persistent synergid	Degenerating	Metabolic activity

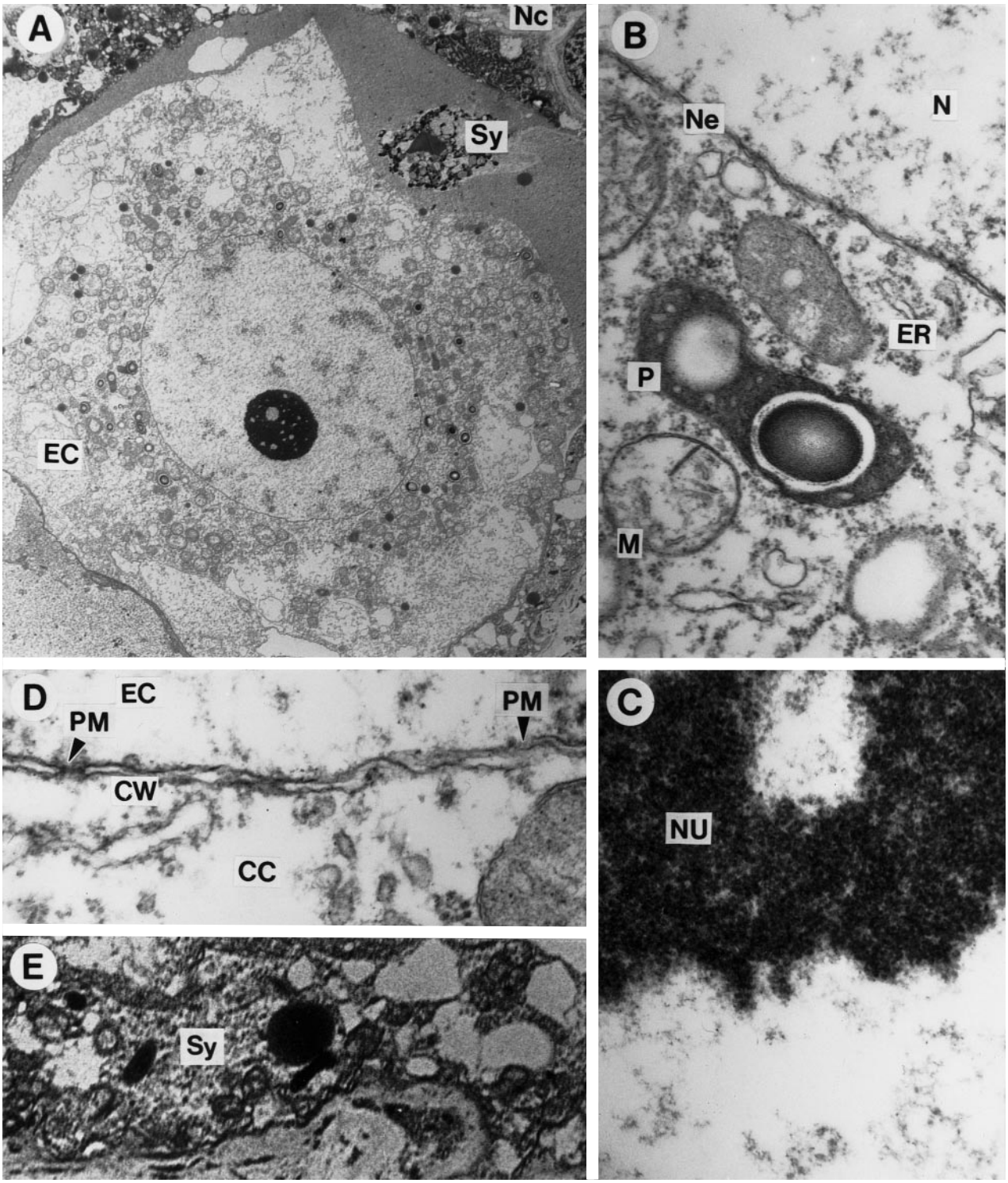

Fig. 1A–E Egg cell of the sexual line (aS) 3 days before anthesis. **A** Survey of the egg cell. ×2100. **B** Details of nucleus and cytoplasm: homogenous chromatin network within the nucleus, rare nuclear pores in nuclear envelope, endoplasmic reticulum of short cisternal phase and sporadically extending in the cytosol, plastids containing starch, mitochondrial matrix poorly developed. ×30 000. **C** Granular component within the peripheral part of nucleolus, without ribosomal subunits, ×66 000. **D** Chalazal part of the egg cell wall becoming interrupted. ×66 000. **E** Fragment of persistent synergid. ×10 000

Abbreviations (for all figures) *CC* central cell, *CW* cell wall, *E* embryo, *EC* egg cell, *ER* endoplasmic reticulum, *G* Golgi apparatus, *L* lipid body, *M* mitochondria, *N* nucleus, *Nc* nucellar epidermis, *Ne* nuclear envelope, *NU* nucleolus, *P* polysomes, *PL* plastid, *PM* plasma membrane, *PN* polar nuclei, *PSy* persistent synergid, *RS* ribosomal subunits, *RSy* receptive synergid, *Sy* synergid, *Z* zygote

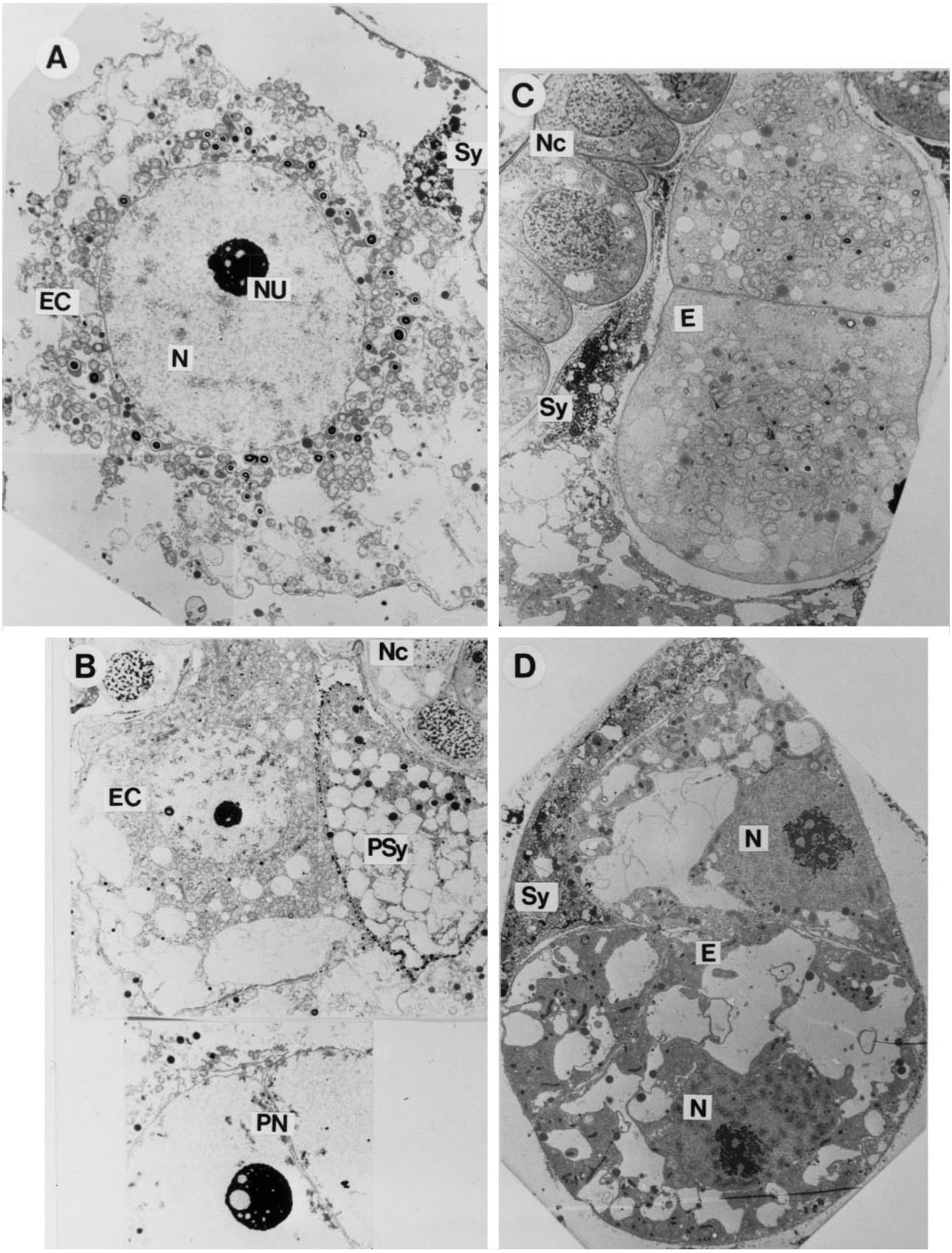

Fig. 2A–D Egg cell and proembryo of the sexual (aS) and parthenogenetic (kS) lines. **A** Egg cell of the sexual line during anthesis. ×1400. **B** Egg cell, persistent synergid and polar nuclei of the parthenogenetic line 3 days before anthesis. ×800 (the diameter of this egg cell corresponds to those in **A**). **C** Sexual two-celled embryo 3 days after anthesis. ×700. **D** Parthenogenetic three-celled embryo 3 days after anthesis, ×700

During anthesis

The egg cell was larger in size than at 3 days before anthesis (Table 1). This was mainly the consequence of vacuolization (Fig. 2A). The egg cell was expanded towards the chalaza, and located chalazally to the synergids. The mature egg cell revealed ultrastructural changes in the nucleus, nucleolus and cytoplasm when compared to 3 days earlier (compare Fig. 1B, D with Fig. 3A,B). The nucleus and nucleolus approximately doubled in diameter. Nuclear pores in the nuclear envelope became more frequent (Fig. 3B). New ribosomal subunits were obviously present in the nucleus (Fig. 3A,B). Short as well as large cisternae of the ER were swollen (Fig. 3A,B). In a few cases the ER lumen was in direct contact with the lumen of the nuclear envelope and with the *cis*-Golgi compartments, which displayed only a few small vesicles (Fig. 3B). Starch granules in plastids and lipid bodies were abundant (Fig. 3A). A regular cell wall was absent at the chalazal end. Only a plasma membrane separated the egg and central cell.

The synergids showed progressive ultrastructural changes. The receptive synergid was highly degraded. Cell organelles were no longer identifiable, and no membranes were visible. The persistent synergid was strongly vacuolized, numerous lipid bodies were present, and only the membrane remnants of mitochondria could be detected (Fig. 3C).

Seventeen hours after pollination

Fusion of the male and female nuclei was complete and a second nucleolus was formed. The nucleus was irregular in shape and contained an active nucleolus (Fig. 3E). Condensation of the chromatin in preparation for nuclear division was observed in the zygote (Fig. 3E). Ribosomes and polysomes were numerous in the cytoplasm (Fig. 3F). The ER occurred more frequently and formed wide, long and branching cisternae (Fig. 3F). Contacts between the ER and nuclear envelope lumena were common. Many Golgi stacks connected to the ER were now present in the cytoplasm. Vesicles of varying size were numerous in the cytosol. The mitochondrial matrix had a high electron density. Fewer starch and lipid bodies were present than at anthesis (Fig. 3D). The cell wall was now completed in the chalazal region.

Ultrastructural peculiarities of the parthenogenetic line (*kotschyi*)-Salmon

Three days before anthesis

The egg cell, its nucleus and nucleolus were larger in the (*kotschyi*)-Salmon (kS) than in the (*aestivum*)-Salmon (aS) line. The size of the kS egg cell at this stage was comparable to that of the aS egg cell at anthesis (Fig. 2A,B; Table 1). Large vacuoles occupied the chalazal region of the cell. Numerous pores were observed in the nuclear envelope. Ribosomes were frequently observed at the outer nuclear membrane and ribosomal subunits were located in the nuclear matrix close to the nuclear pores (Fig. 4A). In contrast to the aS egg cell, a second nucleolus of small size with nucleolar vacuoles and predominating granular components appeared in the kS egg cell (Fig. 2B).

Ribosomes were abundant in the cytosol of the egg cell and mostly aggregated into rosette-like polysomes. They were found either free or attached to the ER membrane. The ER developed long and branching tubules with a wide lumen space (Fig. 4A). Contact of the ER lumen with the lumen of nuclear envelope and with the *cis*-Golgi cisternae occurred frequently. A few plastids contained starch granules; lipid bodies were rare (Fig. 4A). The cell wall was absent for a long distance in the chalazal part of the egg cell where only a plasma membrane was found (Fig. 4B).

The persistent synergid in the kS line was functionally active. Processes of cell organelle degradation were not observed. The receptive synergid showed an advanced degree of degradation. The polar nuclei were located close to the egg apparatus (Fig. 2B).

During anthesis

The egg cell, its nucleus and nucleolus continued to increase in size and were also larger at this stage in the kS line than in the aS line (Fig. 5). The nucleus was located in the centre and the vacuoles were concentrated at the cell periphery. The nuclear envelope had numerous pores (Fig. 4D). Many ribosomes and polysomes were either bound to the nuclear membrane and the membranes of the ER or found free in cytosol. The long cysternal profiles of the ER were abundant and contacted the nuclear envelope and Golgi apparatus frequently (Fig. 4D,E). The organization of the egg cell organelles of the parthenogenetic kS line during anthesis was comparable to that of the zygote of the sexual aS line 17 h after pollination (Fig. 4C,D,E). The cell wall, however, differed between the two lines at these developmental stages. While the cell wall was complete around the zygote, it was absent at the chalazal end of the egg cell of the kS line at anthesis (Fig. 4F).

Fig. 3A–F Details of the egg cell/zygote and synergids of the sexual line (aS) at anthesis (A–C) and 17 h after pollination (**D–F**). **A** Clustered mitochondria and plastids (some with starch granules) are near the nucleus, ×9000. **B** Ribosomal subunits are present in the nuclear matrix, pores are frequently found in the nuclear envelope, ER is characterized by enlarged cisternal profiles, the ER lumen is rarely in contact with the lumen of nuclear envelope, a lipid body is present in cytosol. ×42 000. **C** Persistent synergid, ×5000. **D** Chalazal part of the zygote. ×3750. **E** Nucleus with nucleolus. ×3750. **F** Cytoplasm with a plastid, a long, branching ER cisterna, mitochondria, and numerous ribosomes and polysomes. ×30 000 ▶

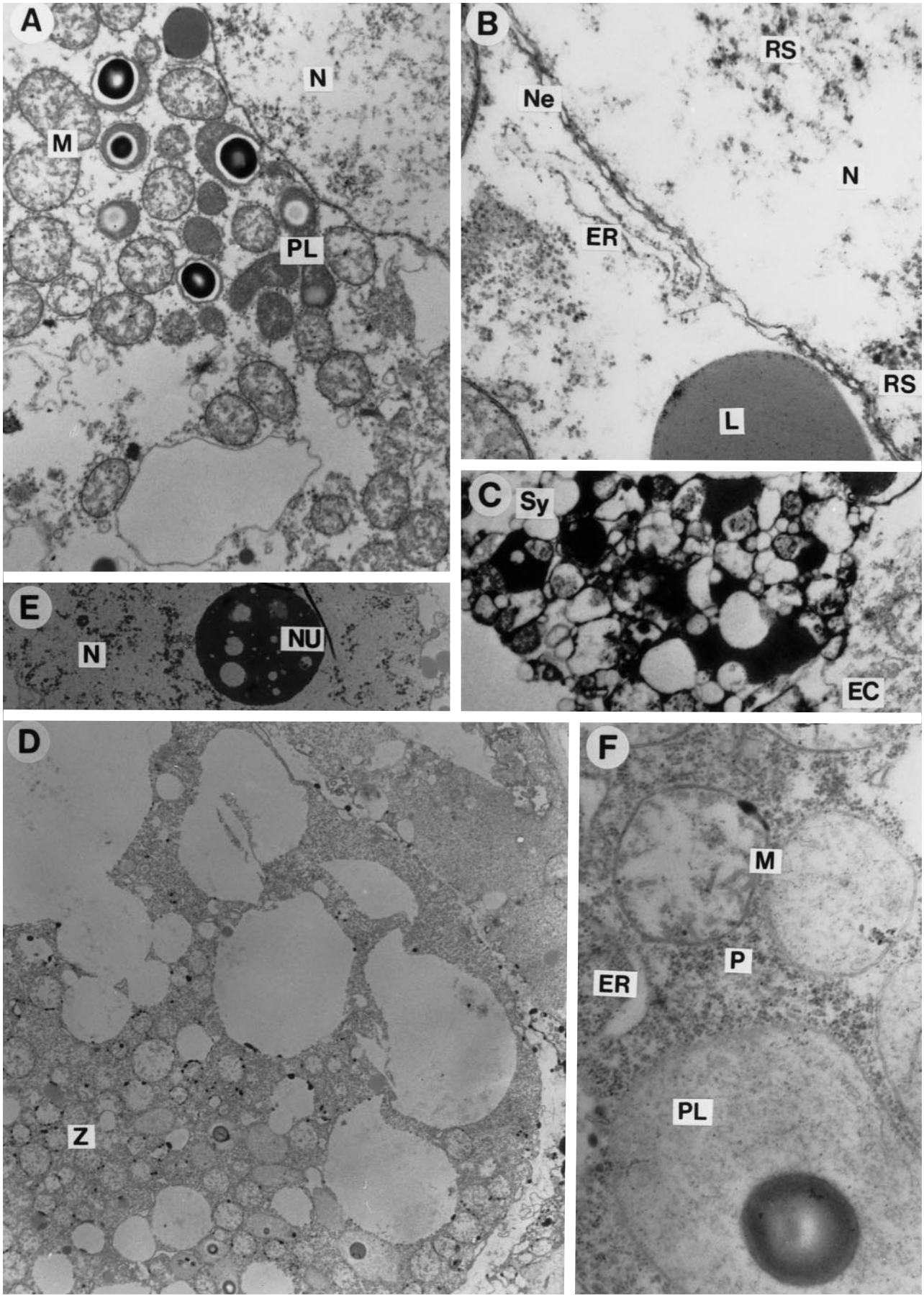
A
N
M
PL
B
RS
Ne
N
ER
RS
L
C
Sy
EC
E
N
NU
D
Z
F
M
P
ER
PL

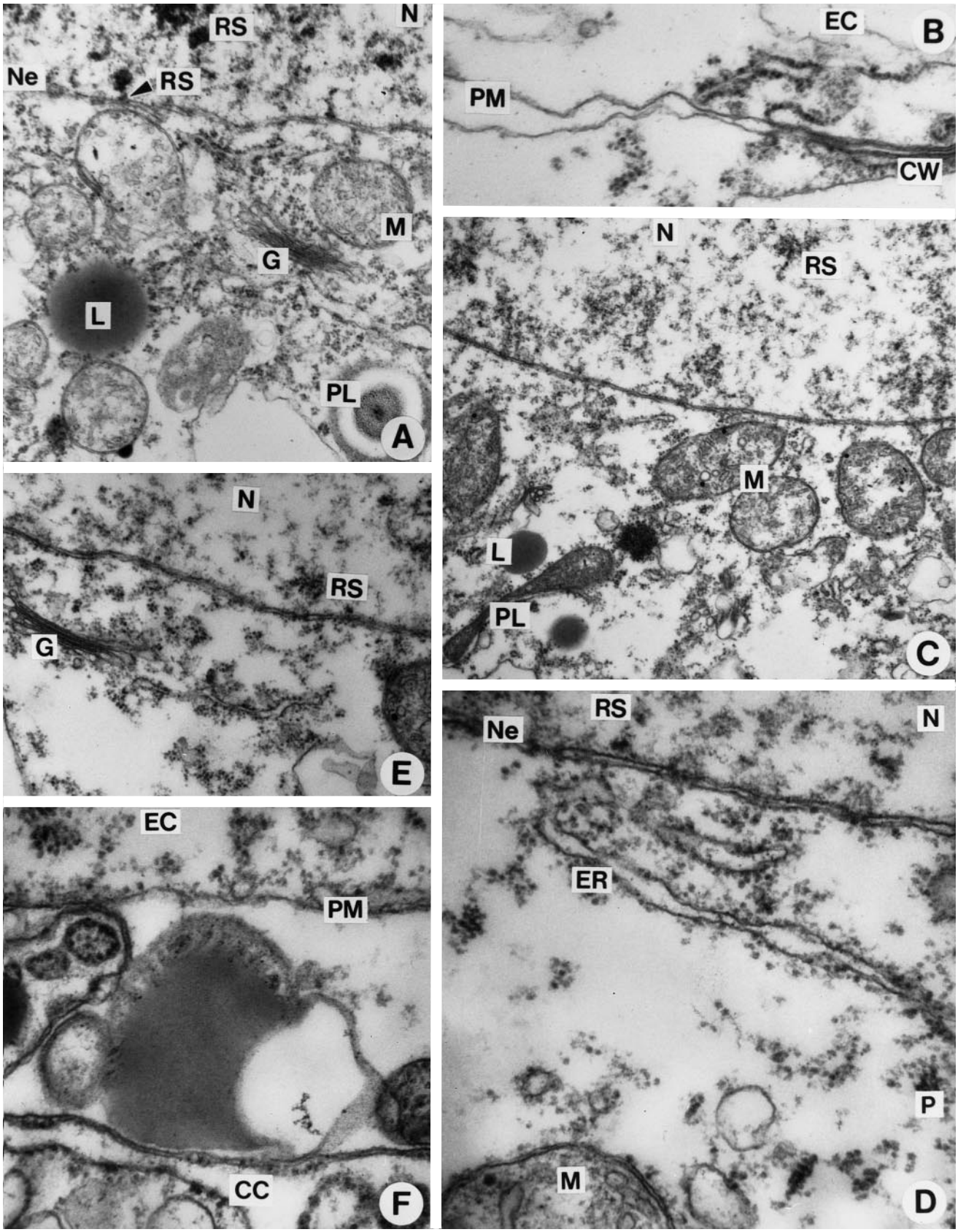

Fig. 4A–F Details of the egg cell of the parthenogenetic (kS) line 3 days before anthesis (**A,B**) and during anthesis (**C–F**). **A** Nucleus and cytoplasm: plastids, mitochondria, lipid bodies, long branching tubules of ER, Golgi stacks, ER lumen in contact with lumen of nuclear envelope and with *cis*-Golgi cisternae. ×30 000. **B** Only a plasma membrane is seen where the cell wall is absent over a long distance at the chalazal end. ×42 000. **C** Nucleus and cytoplasm with several mitochondria, plastids, lipid bodies and numerous free ribosomes, polysomes and vesicles. ×19 500. **D** Long, swollen tubules of ER in contact with nuclear envelope, transport of ribosomal subunits through the nuclear pores. ×66 000. **E** Golgi apparatus close to nucleus. ×30 000. **F** Cell wall absent in chalazal part, only the plasma membrane separates the egg cell from intercellular space and the central cell. ×66 000

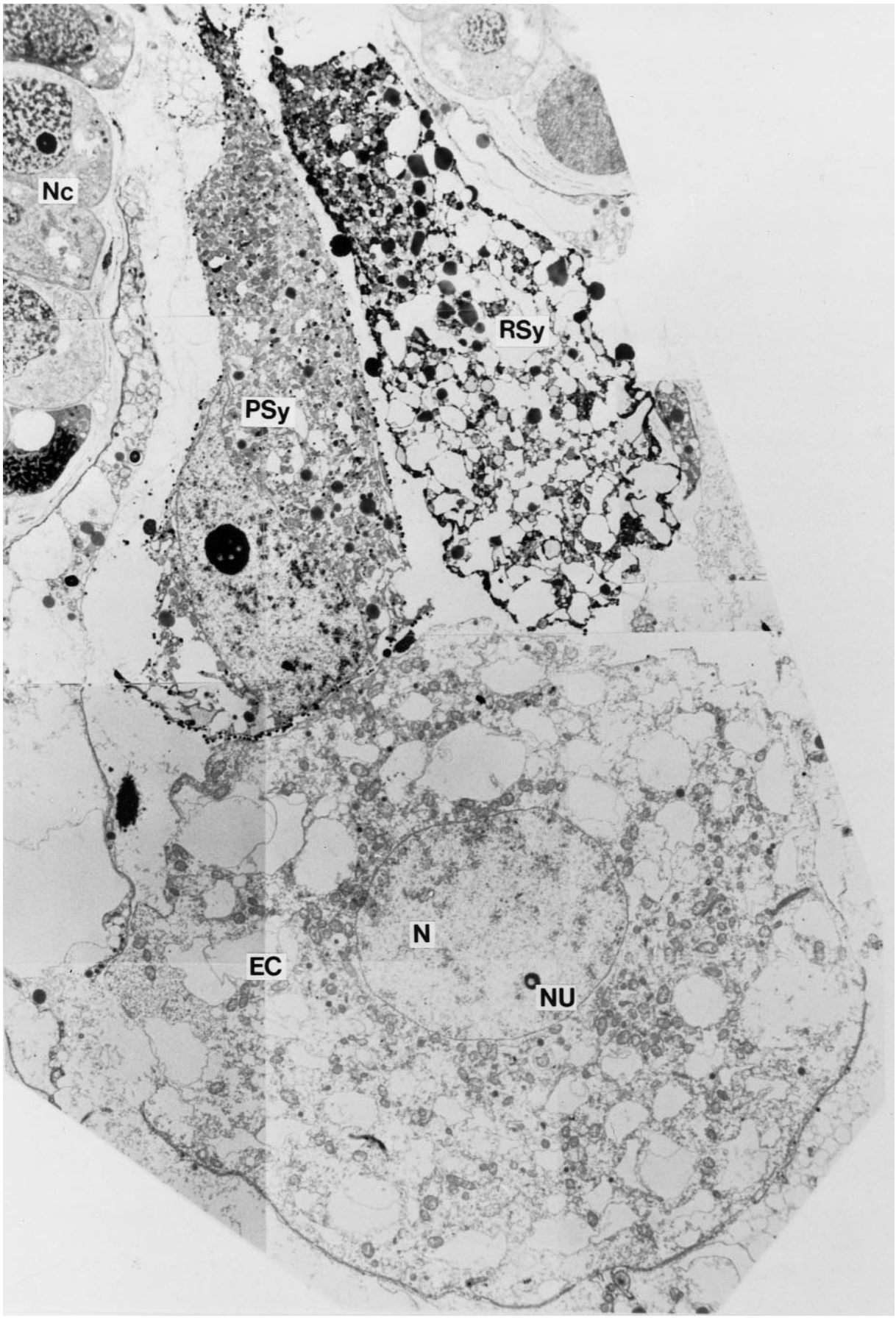

Fig. 5 Egg apparatus of the parthenogenetic (kS) line during anthesis. The egg cell is located chalazally to the synergids, the persistent synergid is metabolically active, and the receptive synergid is in the process of degradation. ×1500

Ultrastructural differences were also found in the synergids of the two lines. In contrast to the sexual line, the persistent synergid of the kS line was metabolically active and free of large vacuoles during anthesis. The nucleus was rather large and of irregular shape. It occupied the chalazal part of the cell. This is unusual for synergids. The nucleolus was large and contained vacuoles. Mitochondria and plastids were very abundant. No starch was found, but lipid bodies were numerous (Fig. 5). The receptive synergid was highly degraded; its cell organelles were no longer recognizable.

Continuation of development of the zygotic and also the parthenogenetic pathway was confirmed by the embryos found in both lines 3 days after anthesis (Fig. 2C,D).

Discussion

Results of the ultrastructural studies revealed significant temporal differences in metabolic activation of the egg cell between the sexual aS and parthenogenetic kS lines (Table 1). A precocious and pollination/fertilization-independent metabolic activation of the egg cell was observed in the parthenogenetic line 3 days before anthesis. Activation of the egg cell is characterized by changes in the fine structure of cell organelles responsible for synthesis, metabolism and transport of proteins. It is recognizable by an increase in the size of the nucleus and nucleolus, the portion of the granular component within the nucleolus, the abundance of ribosomal subunits within the nucleoplasm and their concentration close to the nuclear envelope, the number of nucleoli, the frequency of pores in the nuclear envelope, the abundance of ER profiles and their contacts with the nuclear envelope and Golgi apparatus as well as by an increasing frequency of polysomes within the cytosol.

Vielle et al. (1995) also observed precocious activation of egg cells in apomictic genotypes of *Pennisetum ciliare*; additionally, a complete cell wall around the egg cell hindered the fusion of the male and female gametes. No barriers to fertilization were found in aposporous egg cells of *Panicum maximum* (Naumova and Willemse 1995). For the haploid initiator mutant of barley, Mogensen (1982) assumed that entrance of the sperm into the egg is prevented by some physiological means since there appears to be no structural explanation for why this process is halted. The cell wall structures around the egg cells of the sexual (aS) line and the parthenogenetic (kS) line were identical during anthesis. Only a plasma membrane was present in the chalazal part of both lines. Therefore, the possibility that a physical barrier hinders the fusion of the male and female gametes in the parthenogenetic line may be excluded. The precocious metabolic activation of the egg cell is probably linked with loss of its receptivity while fusion of one sperm with the polar nuclei is still possible. As in previous histological studies (Matzk et al. 1997), proembryos did not occur in the embryo sacs of the parthenogenetic line before or during anthesis. The results of our ultrastructural studies match those of molecular analyses in the Salmon system. An embryo-sac-specific α-tubulin was present in the parthenogenetic line and absent in the sexual isogenic line during the period from 3 days before until 1 day after anthesis (Matzk et al. 1997). In studies that are in progress, where sensitive subtractive hybridization and messenger display techniques are being used, one cDNA clone (MCM2) probably involved in the initiation of DNA replication and cell cycle regulation has been isolated (Bäumlein et al. 1996).

Haploid parthenogenesis in the Salmon system is genetically controlled (Tsunewaki and Mukai 1990). Autonomous embryo development occurs only in the absence of the ‘parthenogenesis-suppressing gene’ (*Spg*) located on the 1 BS-chromosome of wheat and in the presence of both the ‘parthenogenesis-inducing gene’ (*Ptg*) located on the 1 RS-chromosome of rye and a cytoplasmic factor of certain *Aegilops* species. We may speculate about whether the high number and density of ribosomes observed in the egg cell of the kS line before anthesis results from interaction of the *ptg* gene with the alien cytoplasmic factor, and whether the ribosomes are involved in the process of α-tubulin formation within the embryo sac (Matzk et al. 1997). In either case, the observed ultrastructure of the egg apparatus represents intense genetic transcription in the parthenogenetic line already at 3 days before anthesis.

The parthenogenetic pathway could be induced by altered expression of a gene normally involved in sexual reproduction rather than a new regulator gene. This hypothesis was discussed by Nogler (1984) and Koltunow (1992) for the genetic evolution of apomixis. Also, the recently presented “duplicate-gene asynchrony hypothesis” (Carman 1997) points in the same direction. The precocious egg cell activation and the temporal shift of α-tubulin formation may be caused by an asynchrony of nuclear and cytoplasmic gene expression in the parthenogenetic alloplasmic (*kotschyi*)-Salmon line.

Not only egg cells but also synergids differ with respect to their structural features between the sexual aS and parthenogenetic kS lines. The patterns of synergids in the aS line are similar to those described by You and Jensen (1985) and Gao et al. (1992). However, in the kS line the synergids were more active than in the aS line; the receptive synergid degenerated later and the persistent synergid remained active. The persistent synergid is similar to the egg cell in being characterized by a chalazally positioned nucleus, a micropylar vacuole, a very large nucleus and nucleolus, many mitochondria, ER, polysomes and lipid bodies. These conditions may explain the frequent occurrence of additional embryos (twins) in seeds of the parthenogenetic line kS (Tsunewaki and Mukai 1990; Matzk et al. 1995). The haploid partner of a twin probably originates from the precocious activated egg cell developed autonomously and the diploid partner originates from the egg-like synergid fertilized after anthesis. The haploid seedlings are generally more vigorous than the diploids.

Ultrastructural data available about the megagametophyte in sexual wheat are limited to the developmental stages immediately before and after fertilization (You and Jensen 1985, Gao et al. 1992). These results have been confirmed for the sexual Salmon line (aS) at anthesis and 17 h after pollination. Ultrastructural changes of a wheat egg cell associated with its preparation for the

transition from the gametophytic to the sporophytic generation were revealed for the first time by comparing the developmental stages 3 days before anthesis and during anthesis. Three days before anthesis, the egg cell of the sexual line already shows a low metabolic activity that is increased during anthesis. This metabolic activity is indicated by the increase in size of the cell, nucleus and nucleolus as well as higher amounts of ER, ribosomes, dictyosomes, secretion vesicles and vacuoles. This is in contrast to the metabolically inactive mature egg cells of maize (Diboll and Larson 1966), barley (Mogensen 1982) or pearl millet (Taylor and Vasil 1995).

Acknowledgements The authors thank Dr. I. Schubert for critical reading of the manuscript and fruitful discussion, Dr. K. Adler for the facilities of the Electron Microscopy Department, W. Panitz and B. Claus for technical help, and B. Schäfer and H. Ernst for photographic art work.

References

Bäumlein H, Balzer HJ, Borysiuk L, Meyer HM, Matzk F (1996) Gynoeceum specific gene expression in sexual and parthenogenetic wheat lines. In: Proc 14th Int Congr Sex Plant Reprod, Lorne, Australia, 18–23 February, 1996, p 4

Carman JG (1997) Asynchronous expression of duplicate genes in angiosperms may cause apomixis, bispory, tetraspory, and polyembryony. Biol J Linn Soc 61:51–94

Diboll AG, Larson DA (1966) An electron microscope study of the mature megagametophyte in *Zea mays*. Am J Bot 53:391–402

Gao X, Francis D, Ormrod JC, Bennett MD (1992) An electron microscopic study of double fertilization in allohexaploid wheat *Triticum aestivum* L. Ann Bot 70:561–568

Koltunow AM (1992) Apomixis: embryo sacs and embryos formed without meiosis or fertilization in ovules. Plant Cell 5: 1425–1437

Matzk F (1996) The 'Salmon system' of wheat - a suitable model for apomixis research. Hereditas 125:299–301

Matzk F, Meyer HM, Bäumlein H, Balzer HJ, Schubert I (1995) A novel approach to the analysis of the initiation of embryo development in Gramineae. Sex Plant Reprod 8:266–272

Matzk F, Meyer HM, Horstmann C, Balzer HJ, Bäumlein H, Schubert I (1997) A specific α-tubulin is associated with the initiation of parthenogenesis in 'Salmon' wheat lines. Hereditas 126:219–224

Mogensen HL (1982) Double fertilization in barley and the cytological explanation for haploid embryo formation, embryoless caryopses, and ovule abortion. Carlsberg Res Comm 47:313–354

Naumova TN (1993) Apomixis in angiosperms: nucellar and integumentary embryony. CRC Press, Boca Raton

Naumova TN, Willemse MTM (1995) Ultrastructural characterization of apospory in *Panicum maximum*. Sex Plant Reprod 8:197–204

Naumova TN, Den Nijs APM, Willemse MTM (1993) Quantitative analysis of aposporous parthenogenesis in *Poa pratensis* genotypes. Acta Bot Neerl 42:299–312

Nogler GA (1984) Gametophytic apomixis. In: Johri BM (ed) Embryology of angiosperms. Springer, Berlin Heidelberg New York, pp 475–518

Osadtchiy J, Naumova TN (1996) Diplospory in *Poa nemoralis* and *P. palustris*: ultrastructural aspects. Apomixis Newslett 9:6–9

Taylor MG, Vasil IK (1995) The ultrastructure of zygotic embryo development in pearl millet (*Pennisetum glaucum*; Poaceae). Am J Bot 82:205–219

Tsunewaki K, Mukai Y (1990) Wheat haploids through the Salmon method. In: Bajaj YPS (ed) Wheat. (Biotechnology in agriculture and forestry, vol 13). Springer, Berlin Heidelberg New York, pp 460–478

Vielle JP, Burson BL, Bashaw EC, Hussey MA (1995) Early fertilization events in the sexual and aposporous egg apparatus of *Pennisetum ciliare* (L.) Link. Plant J 8:309–316

Yan H, Yang H-Y, Jensen WA (1989) An electron microscope study on in vitro parthenogenesis in sunflower. Sex Plant Reprod 2:154–166

You R, Jensen WA (1985) Ultrastructural observations of the mature megagametophyte and the fertilization in wheat (*Triticum aestivum*). Can J Bot 63:163–178